IEEE Access
Multidisciplinary | Rapid Review | Open Access Journal

Received April 21, 2019, accepted May 2, 2019, date of publication May 9, 2019, date of current version June 7, 2019.

Digital Object Identifier 10.1109/ACCESS.2019.2916005

An Efficient Encoder-Subcarrier Mapping Method Combined With Polar Code for Visible Light Communication

JING HE, KAIQUAN WU, JING HE, ZHIHUA ZHOU, JIE MA, AND JIN SHI
College of Computer Science and Electronic Engineering, Hunan University, Changsha 410082, China

Corresponding author: Jing He (jhe@hnu.edu.cn)

This work was supported in part by the National Natural Science Foundation of China (NSFC) under Grant 61775054 and Grant 61377079, and in part by the Science and Technology Project of Hunan Province under Grant 2016GK2011.

ABSTRACT A spectral efficient light emitting diode (LED)-based visible light communication (VLC) system adopting polar-coded 128 quadrature-amplitude modulations (QAM) orthogonal frequency division multiplexing (OFDM) is experimentally demonstrated. To overcome frequency fading in the VLC system, an encoder-subcarrier mapping method is proposed. The experimental results show that, at a sampling rate of AWG with 150 MSa/s, it can realize error-free transmission with high-spectral efficiency (SE) up to 5.77 bit/s/Hz using the proposed method. Its SE is 1.3 times of the un-coded system adopting 16-QAM. At a sampling rate of 175 MSa/s, its measured Q-factor is 9.86 dB, which improves by 5.12 dB compared to the case without coding.

INDEX TERMS Visible light communication (VLC), orthogonal frequency division multiplexing (OFDM), quadrature-amplitude modulation (QAM), polar code.

I. INTRODUCTION

Visible light communication (VLC) is considered as an appealing technology for its large unlicensed and unused visible light spectrum. Meanwhile, it can provide both illumination and communication services for users [1]. Since the light emitting diodes (LEDs) show advantages of high brightness, reliability, low power consumption and long lifetime, the commercialization of LED-based VLC system becomes feasible in the future [2]. However, LED-based VLC system suffers from limited data rate due to LED's constrained modulation bandwidth [3]. To achieve high data rate transmission, spectral efficient techniques are employed such as high-order quadrature-amplitude modulation (QAM) [4], orthogonal frequency division multiplexing (OFDM) [5], [6], multiple-input multiple-output (MIMO) [7] and non-orthogonal multiple access (NOMA) [8], [9]. In [6], by using OFDM combined with 64-QAM, an RGB-LED-based VLC system can realize high spectral efficiency. In addition, the link of VLC system is susceptible to noises, and forward error correction (FEC) [10], [11] is usually utilized to improve reliability. The conventional FEC codes, such as Reed-Solomon (RS) and low-density parity check code (LDPC), induce the VLC system to have a complicated structure and low transmission efficiency [12]. Polar code, as a provable Shannon capacity-achieving code [13], can avoid the issue. By taking advantage of its simpler coding structure and better error correction performance [14], [15], it is applied to on-off keying (OOK) based dimmable VLC system [12]. In [16], similar to the idea of multi-level decoding, the log-likelihood ratios for QPSK symbols on each subcarrier is calculated separately to help polar code to cope with frequency selective fading in the scenario of MIMO-OFDM. However, for VLC system with high spectral efficiency, polar code combined with high-order QAM-OFDM has seldom been considered.

In this paper, a polar-coded 128-QAM OFDM signal transmission is experimentally demonstrated in VLC system. Because construction of polar code is channel dependent, polar code is not adaptive to fading channels. In order to relieve the damage induced by frequency fading, an encoder-subcarrier mapping method combined with polar code is proposed and experimentally demonstrated. The proposed method takes the diverse reliability of OFDM subcarriers into account in order to improve polar decoding performance. Experimental results show that,

The associate editor coordinating the review of this manuscript and approving it for publication was Jiafeng Xie.

based on this proposed method, it can achieve error-free transmission at a sampling rate of 150 MSa/s. Moreover, at 175 MSa/s, bit error rate (BER) can be improved to 9.29×10^{-4}. The corresponding Q-factor is 9.86 dB, which has been improved by 5.12 dB compared to Q-factor of 4.74 dB in the case without coding.

II. PRINCIPLES

A. POLAR ENCODING FOR M-QAM

At the transmitter, assuming that for one codeword x, the length of binary sequence is K and x is of length N ($N = 2^n$, n is a positive integer). Hence, code rate is $R = K/N$. Before encoding, the information bits are mapped into K information bit locations selected by Gaussian approximation method. The mapped bit sequence u then goes through a polarization process to generate x. It can be represented as:

$$x = u \cdot G_N \tag{1}$$

where $G_N \triangleq B_N \cdot F^{\otimes n}$ represents the encoding matrix. Furthermore, B_N denotes the bit-reversal matrix and $F^{\otimes n}$ represents n-fold Kronecker product of Arikan's standard 2×2 polarizing kernel. The order of M-QAM is $m = \log_2 M$, thus a QAM symbol consists of m bits. To carry out mapping from coded bit sequence into QAM symbols, each codeword x with length of N is divided into N/m blocks. Subsequently, these blocks are mapped into QAM symbols by Gray labeling in order. However, as certain QAM modulation is implemented, e.g. 128-QAM ($m = 7$), $N = 2^n$ is not an integer multiple of m. To be compatible with them, a scheme that combines the standard polarizing kernel with an elaborately designed 7×7 kernel is recommended [17], but it will burden code construction and decoding with high complexity. In the paper, zero-padding suffix is adopted as an alternate approach. Each codeword is suffixed a group of bits '0' so that the last block of bits can be mapped into a QAM symbol. Assuming that the length of one codeword with zero padding suffix is denoted as N_p, thus $N_p - N = m - (N \bmod m)$, and N_p/m QAM symbols are generated.

B. POLAR DECODING FOR M-QAM

As for decoding of received polar coded data, successive cancellation list decoding (SCL) algorithm is carried out [18]. Its soft-decision decoding is implemented based on log-likelihood ratios (LLRs). LLRs are calculated by soft demodulator containing all the probability information of each bit. Considering a group of received N_p/m M-QAM symbols, the p-th $p = 1, 2, \cdots, N_p/m$ received M-QAM symbol is labeled as $y_p = y_{p,\mathrm{Re}} + i \cdot y_{p,\mathrm{Im}}$. Its transmitted counterpart is labeled as $x_k^{q,b} = x_{k,\mathrm{Re}}^{q,b} + i \cdot x_{k,\mathrm{Im}}^{q,b}$, ($k = 1, 2, \cdots, 2^{m-1}$), whose q-th($q = 1, 2, \cdots, m$) bit of the QAM symbol is b (0 or 1) with 2^{m-1} cases, i.e. $x_{(p-1)\cdot m+q} = b$. The calculation of prior probability can be measured as

$$\begin{aligned} &P(y_p|x_{(p-1)\cdot m+q} = b) \\ &= \sum_{k=1}^{2^{m-1}} p(y_{p,\mathrm{Re}}, x_{k,\mathrm{Re}}^{q,b}) \cdot p(y_{p,Im}, x_{k,Im}^{q,b}) \\ &= \sum_{k=1}^{2^{m-1}} \frac{1}{2\sigma^2\pi} \exp\left(-\frac{\left(y_{p,\mathrm{Re}} - x_{k,\mathrm{Re}}^{q,b}\right)^2 + \left(y_{p,Im} - x_{k,Im}^{q,b}\right)^2}{\sigma^2}\right) \end{aligned} \tag{2}$$

The variance σ^2 of additive white Gaussian noise can be obtained given the subcarrier's SNR, based on the channel state information (CSI). Because the bit '0' and '1' tend to appear with the same probability in the source data, we can exploit the relationship below,

$$P(y_p|x_{(p-1)\cdot m+q} = 1) = P(y_p|x_{(p-1)\cdot m+q} = 1) = \frac{1}{2} \tag{3}$$

Thus, with the knowledge of Bayes's theorem and the equation above the posterior probability is obtained as shown below,

$$\begin{aligned} &P(x_{(p-1)\cdot m+q} = b|y_p) \\ &= \frac{P(y_p|x_{(p-1)\cdot m+q} = b) \cdot P(x_{(p-1)\cdot m+q} = b)}{P(y_p)} \\ &= \frac{P(y_p|x_{(p-1)\cdot m+q} = b)}{P(y_p|x_{(p-1)\cdot m+q} = 0) + P(y_p|x_{(p-1)\cdot m+q} = 1)} \end{aligned} \tag{4}$$

Then the corresponding LLR of the q-th bit in p-th M-QAM symbol is defined as,

$$LLR_{p\cdot m+q} = \ln \frac{P(x_{(p-1)\cdot m+q} = 1|y_p)}{P(x_{(p-1)\cdot m+q} = 0|y_p)} \tag{5}$$

Then N_p LLRs are output from soft QAM demodulator, and those for zero padding suffix is punctured. Subsequently, N LLRs are fed into polar decoder to help SCL to choose the most reliable decoding path in L candidate paths.

C. AN ENCODER-SUBCARRIER MAPPING METHOD FOR OFDM VLC CHANNEL

For OFDM modulation, the subcarriers can be regarded as multi-channels. The conventional subcarrier mapping method puts consecutive part of data on separated data subcarriers before carrying out inverse fast Fourier transform (IFFT), which is shown in Fig. 1(a). For instance, assuming that the number of OFDM symbols per frame is N_s, and $Z_{e,f}$ denotes the f-th ($f = 1, 2, \cdots, N_s$) OFDM symbol in the e-th ($e = 1, 2, \cdots, N_{DC}$) data subcarrier, to fully load data into these subcarriers, the $((e-1)\cdot N_{DC} + f)$-th QAM symbol is placed in the order of $Z_{1,1}, Z_{2,1}, \cdots, Z_{N_{DC},1}, \cdots\cdots, Z_{1,N_S}, Z_{2,N_S}, \cdots, Z_{N_{DC},N_S}$. This method is acceptable when the system is free of the frequency fading effect [19], [20]. Because polar code simplifies the noise as additive white Gaussian noise (AWGN), and data subcarriers nearly suffer from noises to the same extent that can be treated uniformly by polar decoder. As a result, the reliability of received bits can simply be measured by the electrical SNR of the signal.

As mentioned above, one feature of polar code construction is channel dependent, hence it is not versatile for fading channels because of mismatched decoding. Unfortunately, the transmission of VLC system suffers from a fading effect, incurring severe damages to high-frequency

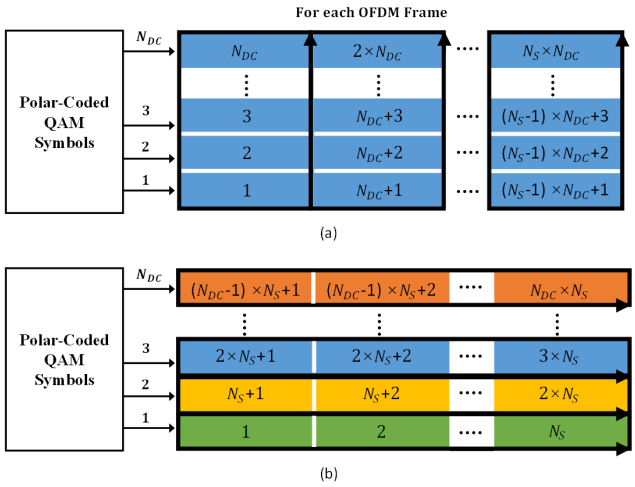

FIGURE 1. **(a) The polar-coded scheme with conventional subcarrier mapping and (b) the proposed encoder-subcarrier mapping method combined with polar code.**

subcarriers [11]. It is mainly caused by the limited bandwidth of devices such as LED and photodiode (PD). As a consequence, the channel model cannot be regarded as an invariant AWGN channel if the conventional subcarrier mapping method is applied. Hence, it indicates that LLRs of each subcarrier should be treated independently according to its SNR. To solve the problem, an encoder-subcarrier mapping method combined with polar code is proposed in the paper. Unlike the conventional subcarrier mapping method, which assigns one unified encoder's output to different subcarriers in the environment of various degree of noises, the proposed method assigns one encoder to each specific subcarrier as shown in Fig. 1(b). According to the method, the data subcarriers are loaded with data from the same encoder one at a time, and the QAM symbols are placed as $Z_{1,1}, Z_{1,2}, \cdots, Z_{1,N_S}, \cdots\cdots, Z_{N_{DC},1}, Z_{N_{DC},2}, \cdots, Z_{N_{DC},N_S}$. For polar decoding, by using CSI of data subcarrier separately, the corresponding LLR of each bit is measured through soft demodulation accurately.

As for code construction, it has been concluded that one optimized design SNR can provide nearly the best performance across a range of SNRs [21]. In our work, encoders share the same designed operating SNR. Thus, the only difference between the proposed method and the conventional method is the pattern of QAM symbol assigned on subcarriers. Therefore, better decoding performance is obtained without extra computational cost.

III. EXPERIMENTAL SETUP AND RESULTS

To evaluate the performance of the 128-QAM OFDM VLC system aided by polar code based on encoder-subcarrier mapping method, the experimental setup is shown in Fig. 2. At the transmitter, digital signal processing (DSP) is carried out offline in MATLAB. At first, serial to parallel conversion is implemented, and then the data is polar encoded and mapped into 128-QAM symbols. The code length of polar code N is chosen as 512 with code rate R of 0.5, and accordingly, N_p is 518 and K is 256. After mapping QAM symbols into each subcarrier, the random interleaver shuffles the symbols in each subcarrier to avoid burst error as well as reduce peak-to-average power ratio (PAPR) of the signal. The IFFT size N_{IFFT} is 128, of which in total N_{DC} of 57 subcarriers are used to carry data and the rest subcarriers are set to null. It can mitigate ground noise. Subsequently, cyclic prefix (CP) with length N_{CP} of 16 is inserted. After parallel to serial conversion, training sequences (TS) are added in each frame for synchronization and channel estimation. To obtain an accurate estimation of SNRs for subcarriers, another independent TS is sent in advance. The signal carrying the sum of 1036 OFDM symbols is then loaded into arbitrary waveform generator (AWG, Tektronix 7122C) with peak-to-peak voltage of 0.5 V. Then, to obtain the best performance, the signal is amplified by an electrical amplifier (EA) with voltage of 23.72 V and biased at 3.23 V. Subsequently, it is injected to a commercially available blue-ray LED with bandwidth (BW_{LED}) of 80 MHz.

At the receiver, the signal is received by a PD after 50-cm free space transmission and amplified by a trans-impedance amplifier (TIA). The digital storage oscilloscope (DSO, Tektronix TDS6804B) is adopted to oversample the electric signal at a sampling rate of 2.5 GSa/s. Then offline DSP includes synchronization, fast Fourier transform (FFT), channel equalization, de-interleaving, and subcarrier demapping. After subcarrier de-mapping, received QAM symbols for each subcarrier are obtained. Based on estimated SNR for each data subcarrier with the help of the independent TS, M-QAM soft demodulation is carried out to yield LLRs for polar decoder. Finally, the decoded bits are collected subcarrier by subcarrier to recover the data.

The insets of Fig. 2 also show the experimental results at the AWG sampling rate of 175 MSa/s. The estimated SNR of corresponding data subcarrier is illustrated in Fig. 2(a). In order to give a better equalization performance, intra-symbol frequency-domain averaging (ISFA) algorithm [22] is adopted. It smooths the channel response over all subcarriers, which is illustrated in Fig.2 (b) that also indicates the frequency fading effect. Although there is radical fluctuation among the SNR of subcarriers, it can be observed that higher-frequency subcarriers suffer from severer fading effect. For data subcarriers, the SNR gap between the lowest and highest reaches up to 16 dB, while the average SNR is only 18.28 dB. Moreover, Fig.2 (c) and (d) shows the power spectral density (PSD) of the transmitted signal and the received signal, respectively. The attenuation caused by VLC transmission along with devices such as AWG, PD and OSC suppress the PSD of the received signal.

In addition, to investigate how sampling rate of AWG affects the overall SNR, 5 different values from 100 MSa/s to 200 MSa/s of AWG sampling rate, in step value of 25 MSa/s are measured. Since the modulated bandwidth of LED is

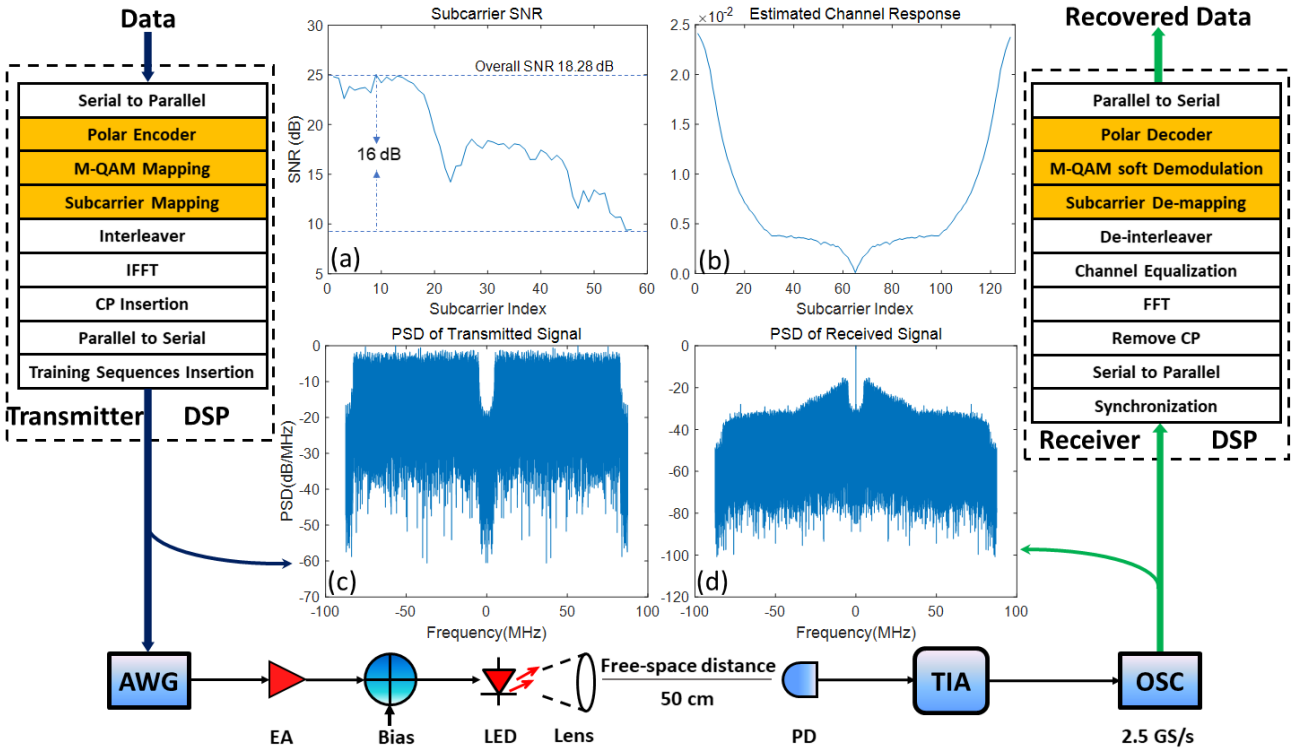

FIGURE 2. The experimental setup for 128-QAM at sampling rate of 175 MSa/s scenario, (a) the estimated subcarriers' SNR and (b) the experimental estimated channel response, (c) the power spectral density (PSD) of the transmitted signal, (d) and the PSD of the received signal.

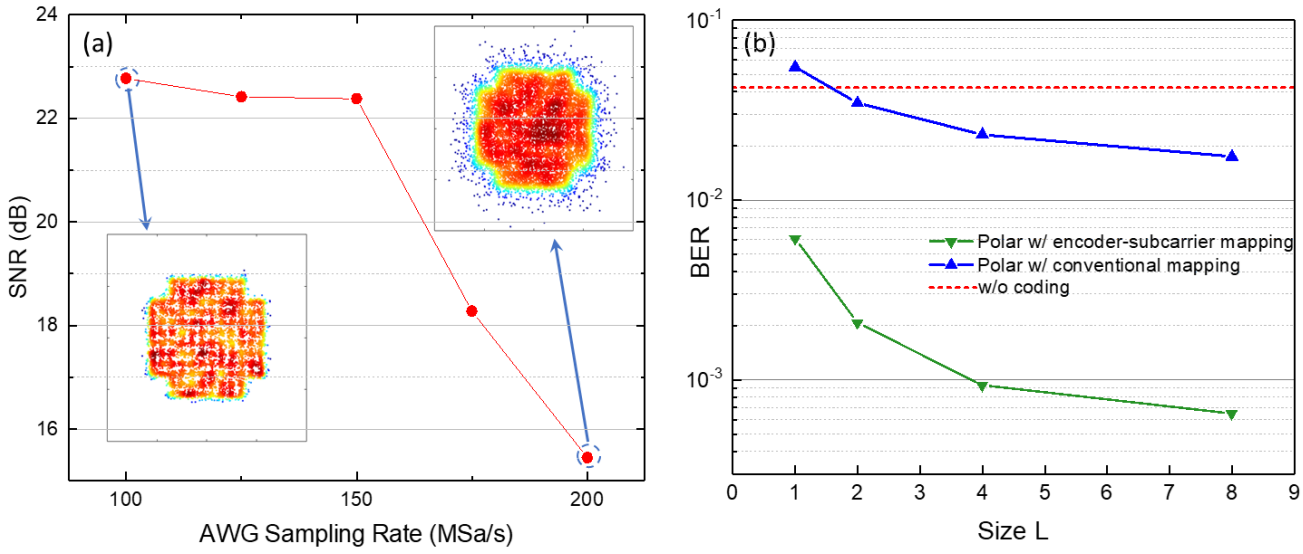

FIGURE 3. Experimental results of (a) SNR versus different sampling rates and two received constellations. (b) BER performance over different SCL decoding list size L with two subcarrier mapping method at a sampling rate of 175 MSa/s.

only 80 MHz, the maximum symbol rate across a bandwidth-limited baseband channel is 160 MSa/s according to Nyquist rate. Sampling rate larger than that will cause inter-symbol interference (ISI). Fig. 3(a) shows that, as sampling rate of AWG increases, the SNR reduces greatly from 22.77 dB to 15.45 dB, where the sampling bandwidth exceeds the modulation bandwidth of LED. Fig. 3(b) illustrates the BER performance over the different list size L for SCL algorithm at sampling rate of AWG with 175 MSa/s. It can be seen that the list size L for SCL algorithm has an impact on its BER performance. For encoder-subcarrier mapping method combined with polar code, the BER is 9.29×10^{-4} while L is 4, which is much better than L of 1 and 2. It reaches the tradeoff between decoding complexity and

TABLE 1. The comparison of BER performance for different schemes.

Sampling Rate (MSa/s)	128-QAM			16-QAM
	Polar w/ encoder-subcarrier mapping	Polar w/ conventional subcarrier mapping	w/o coding	w/o coding
100	0	0	8.79×10^{-3}	0
125	0	0	1.84×10^{-2}	6.85×10^{-5}
150	0	3.89×10^{-4}	2.61×10^{-2}	1.37×10^{-4}
175	9.29×10^{-4}	2.31×10^{-2}	4.21×10^{-2}	9.89×10^{-3}
200	1.37×10^{-1}	2.72×10^{-1}	8.01×10^{-2}	2.58×10^{-2}

TABLE 2. The maximum achievable spectral efficiency.

Parameters/Value	128-QAM polar w/ encoder-subcarrier mapping	16-QAM w/o coding
S (the maximum achievable rate, MSa/s)	150	100
N_{DC}	57	57
N_{IFFT}	128	128
N_{CP}	16	16
m (bit)	7	4
K/N_{pad}	$256/518 \approx 0.494$	1
BW_{LED} (MHz)	80	80
SE (bit/s/Hz)	≈ 5.77	≈ 4.44

BER performance since the performance improvement for L of 8 is negligible. To quantify BER performance, Q-factor is measured according to $Q(dB) = 20\log_{10}[2^{1/2}\text{erfc}^{-1}(2 \cdot BER)]$ [19]. At sampling rate of 175 MSa/s, Q-factor of the encoder-subcarrier mapping method is 9.86 dB, which improves by 3.87 dB compared to the conventional subcarrier mapping, and 5.12 dB compared to the case without coding.

Table 1 presents the comparison of BER performance for three schemes in 128-QAM OFDM-VLC system, i.e. the encoder-subcarrier mapping method combined with polar code, the polar-coded scheme with the conventional subcarrier mapping and the scheme without coding for reference. As sampling rate of AWG increases from 100 MSa/s to 200 MSa/s, the BER performance of the case without coding is incapable of reaching BER at 1×10^{-3}. On the other hand, the BER performance for both polar-coded schemes can avoid error events at sampling rate of AWG lower than 125 MSa/s. However, at sampling rate of AWG with 200 MSa/s, the BER performance of both polar-coded schemes is worse than that of the case without coding. It is resulted from error propagation of the serial decoding feature of SCL [23]. Moreover, as sampling rate of AWG decreases to 175 MSa/s and 150 MSa/s, the BER performance using the encoder-subcarrier mapping combined with polar code is better than that of other two methods. And the encoder-subcarrier mapping method achieves error-free transmission at sampling rate of 150 MSa/s.

Table 1 also shows that for the un-coded system at sampling rate of 100 MSa/s, only the maximum order of 16-QAM can be adopted to achieve error-free transmission. By contrast, polar code can guarantee error-free transmission via 128-QAM at 150 MSa/s for the system with low computation complexity. In addition, spectral efficiency (SE) of the 128-QAM OFDM-VLC system is up to 5.77 bit/s/Hz according to

$$\text{SE} = \frac{S \times (N_{DC}/(N_{IFFT} + N_{CP})) \times m \times (K/N_p)}{\text{BW}_{LED} \times (N_{DC}/N_{IFFT})} \quad (6)$$

where S is the sampling rate [24]. As shown in Table 2, although with the overheads on frozen bits, its SE is still 1.3 times of the un-coded 16-QAM OFDM-VLC system.

IV. CONCLUSION

In this paper, we focus on the optimization of the polar coded modulation for VLC system, and the proposed method can effectively improve its spectral efficiency. A highly spectral efficient polar-coded 128-QAM OFDM-VLC system is experimentally demonstrated. Due to the channel state diversity across OFDM subcarriers induced by frequency fading in VLC system, an encoder-subcarrier mapping method is proposed to avoid mismatched LLRs for polar decoder. Based on the mapping method combined with polar code, the spectral efficiency for the 128-QAM OFDM-VLC system can reach up to 5.77 bit/s/Hz with error-free transmission at sampling rate of 150 MSa/s. Its SE is 1.3 times of the

un-coded system adopting 16-QAM with nearly zero BER. Meanwhile, its BER also achieves to 9.29×10^{-4} at sampling rate of 175 MSa/s, whose Q-factor reaches to 9.86 dB and improves by 5.12 dB in contrast to the case without coding.

The main challenge of the proposed method is the increased processing time delay. Since the data output by one polar encoder are assigned on one subcarrier in different time slots, the decoder needs to wait to obtain a whole received codeword. For example, assuming 2^m-QAM is employed, decoding is performed only after N_p/m OFDM symbols are received. By contrast, the conventional method only requires at least $N_p/(m{\cdot}N_{DC})$ OFDM symbols to perform decoding.

REFERENCES

[1] A. Jovicic, J. Li, and T. Richardson, "Visible light communication: Opportunities, challenges and the path to market," *IEEE Commun. Mag.*, vol. 51, no. 12, pp. 26–32, Dec. 2013.
[2] L. Grobe and A. Paraskevopoulos, "High-speed visible light communication systems," *IEEE Commun. Mag.*, vol. 51, no. 12, pp. 60–66, Dec. 2013.
[3] H. Le Minh *et al.*, "100-Mb/s NRZ visible light communications using a postequalized white LED," *IEEE Photon. Technol. Lett.*, vol. 21, no. 15, pp. 1063–1065, Aug. 1, 2009.
[4] Y. Wang, X. Huang, J. Zhang, Y. Wang, and N. Chi, "Enhanced performance of visible light communication employing 512-QAM N-SC-FDE and DD-LMS," *Opt. Express*, vol. 22, no. 13, pp. 15328–15334, 2014.
[5] R. Deng, J. He, Z. Zhou, J. Shi, M. Hou, and L. Chen, "Experimental demonstration of software-configurable asynchronous real-time OFDM signal transmission in a hybrid fiber-VLLC system," *IEEE Photon. J.*, vol. 9, no. 1, Feb. 2017, Art. no. 7801008.
[6] Y. Wang *et al.*, "875-Mb/s asynchronous bi-directional 64QAM-OFDM SCM-WDM transmission over RGB-LED-based visible light communication system," in *Proc. Opt. Fiber Commun. Conf. Expo. Nat. Fiber Optic Eng. Conf.*, Mar. 2013, pp. 1–3, Paper OTh1G.3.
[7] A. H. Azhar, T. A. Tran, and D. O'Brien, "A gigabit/s indoor wireless transmission using MIMO-OFDM visible-light communications," *IEEE Photon. Technol. Lett.*, vol. 25, no. 2, pp. 171–174, Jan. 2013.
[8] H. Marshoud, V. M. Kapinas, G. K. Karagiannidis, and S. Muhaidat, "Non-orthogonal multiple access for visible light communications," *IEEE Photon. Technol. Lett.*, vol. 28, no. 1, pp. 51–54, Jan. 1, 2016.
[9] C. Chen, W.-De Zhong, H. Yang, and P. Du, "On the performance of MIMO-NOMA-based visible light communication systems," *IEEE Photon. Technol. Lett.*, vol. 30, no. 4, pp. 307–310, Feb. 15, 2018.
[10] S. Kim, "Adaptive FEC codes suitable for variable dimming values in visible light communication," *IEEE Photon. Technol. Lett.*, vol. 27, no. 9, pp. 967–969, May 1, 2015.
[11] Y. Wei, J. He, R. Deng, J. Shi, S. Chen, and L. Chen, "An approach enabling adaptive FEC for OFDM in fiber-VLLC system," *Opt. Commun.*, vol. 405, pp. 329–333, Dec. 2017.
[12] J. Fang *et al.*, "An efficient flicker-free FEC coding scheme for dimmable visible light communication based on polar codes," *IEEE Photon. J.*, vol. 9, no. 3, Jun. 2017, Art. no. 7903310.
[13] E. Arıkan, "Channel polarization: A method for constructing capacity-achieving codes for symmetric binary-input memoryless channels," *IEEE Trans. Inf. Theory*, vol. 55, no. 7, pp. 3051–3073, Jul. 2009.
[14] I. Tal and A. Vardy, "How to construct polar codes," *IEEE Trans. Inf. Theory*, vol. 59, no. 10, pp. 6562–6582, Oct. 2013.
[15] T. Koike-Akino, Y. Wang, S. C. Draper, K. Sugihara, and W. Matsumoto, "Bit-interleaved polar-coded OFDM for low-latency M2M wireless communications," in *Proc. IEEE Int. Conf. Commun.*, May 2017, pp. 1–7.
[16] K. Watanabe, S. Higuchi, K. Maruta, and C.-J. Ahn, "Performance of polar codes with MIMO-OFDM under frequency selective fading channel," in *Proc. 20th Int. Symp. Wireless Pers. Multimedia Commun. (WPMC)*, Bali, Indonesia, 2017, pp. 107–111.
[17] H. Mahdavifar, M. El-Khamy, J. Lee, and I. Kang, "Polar coding for bit-interleaved coded modulation," *IEEE Trans. Veh. Technol.*, vol. 65, no. 5, pp. 3115–3127, May 2016.
[18] I. Tal and A. Vardy, "List decoding of polar codes," in *Proc. IEEE Int. Symp. Inf. Theory* Jul./Aug. 2011, pp. 1–5.
[19] L. Liu *et al.*, "High performance and cost effective CO-OFDM system aided by polar code," *Opt. Express*, vol. 25, no. 3, pp. 2763–2770, 2017.
[20] L. Liu, S. Xiao, M. Bi, J. Fang, Y. Zhang, and W. Hu, "Performance evaluation of high-speed polar coded CO-OFDM system with nonlinear and linear impairments," *IEEE Photon. J.*, vol. 9, no. 4, Aug. 2017, Art. no. 7202909.
[21] H. Vangala, E. Viterbo, and Y. Hong, "A comparative study of polar code constructions for the AWGN channel," Jan. 2015, *arXiv:1501.02473*. [Online]. Available: https://arxiv.org/abs/1501.02473
[22] J. He, T. Li, X. Wen, M. Chen, and L. Chen, "An ISFA-combined pilot-aided channel estimation scheme in multiband orthogonal frequency division multiplexing ultra-wideband over fiber system," in *Proc. IEEE Symp. Comput. Commun. (ISCC)*, Larnaca, Cyprus, Jul. 2015, pp. 913–917.
[23] K. Niu, K. Chen, J. Lin, and Q. T. Zhang, "Polar codes: Primary concepts and practical decoding algorithms," *IEEE Commun. Mag.*, vol. 52, no. 7, pp. 192–203, Jul. 2014.
[24] J. He, H. Dong, R. Deng, T. Li, and L. Chen, "Enhanced performance of CAP system using an overlap frequency-domain equalization scheme," *IEEE Photon. J.*, vol. 8, no. 2, Apr. 2016, Art. no. 6600308.

JING HE received the B.Sc., M.Sc., and Ph.D. degrees from Hunan University, China, in 1999, 2004, and 2009, respectively, where she is currently an Associate Professor with the College of Computer Science and Electronic Engineering, Hunan University. She was an Academic Scholar with Bristol University, U.K., in 2012. Her research interests include modulation format, radio-over-fiber systems, optical signal processing, broadband optical communication, real-time optical communication, and visible light communication.

KAIQUAN WU received the bachelor's degree in communication engineering from Hunan University, China, in 2016, where he is currently pursuing the master's degree. His research interests include optical/fiber communication, channel coding and modulation, and constellation shaping.

JING HE received the bachelor's degree in communication engineering from Hunan University, China, in 2017, where she is currently pursuing the Ph.D. degree. Her research interests include visible light communication, optical camera communication, and signal processing.

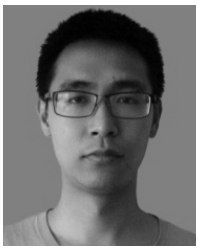

ZHIHUA ZHOU received the master's degree in communication engineering from Hunan University, China, in 2015, where he is currently pursuing the Ph.D. degree. His research interests include optical communication, passive optical networks, and optical signal processing.

JIE MA received the master's degree from the College of Electronic Information and Engineering, Hebei University of Technology, China, in 2017. She is currently pursuing the Ph.D. degree with the College of Computer Science and Electronic Engineering, Hunan University, China. Her research interests include optical communications, passive optical networks, and digital signal processing.

JIN SHI received the bachelor's degree in electronic and information engineering from the Hunan Institute of Science and Technology, China, in 2015. He is currently pursuing the Ph.D. degree from Hunan University. His research interests mainly include optical camera communication, optical real-time communications, and advanced modulation formats.